Numerical simulations of convective bursts occurred just before landfall of Typhoon Lionrock (2016)

*Akiyoshi Wada and Ryo Oyama
[1]Meteorological Research Institute, Tsukuba, Ibaraki, 305-0052, JAPAN
*awada@mri-jma.go.jp

1. Introduction

Typhoon Lionrock was the ninth tropical cyclone in the typhoon season of 2016. According to the Regional Specialized Meteorological Center (RSMC) Tokyo best track analysis, the typhoon was generated around 29.2˚N, 133.3˚E at 1200 UTC on 21 August 2016 and reached the minimum central pressure of 940 hPa around 27.7 ˚N, 137.9˚E at 0600 UTC on 28 August. Then, the typhoon made landfall in the northern region of Japan just before 1200 UTC on 30 August (http://web.archive.org/web/20160830092234/http://www.jma.go.jp/jp/typh/D20160830090017754.html).

During the mature phase of Lionrock that was moving northwestward, Himawari-8 infrared channel (10.4 μm) temperature brightness images captured convective bursts ahead of the typhoon that occurred on the downstream side. In order to clarify the formation process of the precipitation pattern, numerical simulations were performed by using a nonhydrostatic atmosphere model coupled with ocean and ocean wave models (CPL: Wada, 2010).

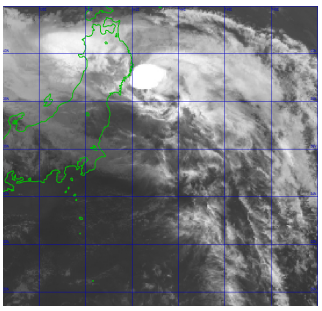

Figure 1 Himawari-8 infrared channel (10.4 μm) temperature brightness image at 0730 UTC on 30 August.

2. Data and method

Figure 2 shows the computational domain. It covered a 3000 km x 3000 km area with a horizontal grid spacing of 3 km. The integration time was 210 hours with the time steps of 3 seconds in the nonhydrostatic atmosphere model, 18 seconds in the ocean model and 10 minutes in the ocean wave model in the CPL. The initial time was 0000 UTC on 23 August in 2016. The nonhydrostatic atmosphere model had 55 vertical levels with variable intervals from 40 m from the near-surface layer to 1013 m for the uppermost layer. The top height was ~26 km. The simulations used the Japan Meteorological Agency global objective analysis data for atmospheric initial and boundary conditions (with a horizontal grid spacing of ~20km) and the daily oceanic reanalysis data calculated by the Meteorological Research Institute multivariate ocean variational estimation (MOVE) system (Usui, et al. 2006) with a horizontal grid spacing of 0.5˚. The interval of model output was 1 hour from the initial time to 108 hours and was 20 minutes after 108 hours.

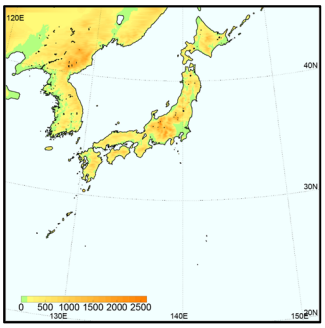

Figure 2 Computational domain. Colors indicate land elevation.

3. Results

3.1 Track and central-pressure simulation

Figure 3a shows the results of track simulations for Lionrock with central pressures simulated by the CPL together with RSMC best track data. According to RSMC best track data, the Lionrock moved southwestward and then changed the direction to eastward and then moved northeastward. The typhoon again changed the direction to north northwestward and then made landfall in the northen region of Japan. The track was successfully simulated by the CPL. Figure 3b showed the time series of best track central pressures and central pressures simulated by the CPL. The best track data indicated that Lionrock underwent rapid intensification from the initial time to 1800 UTC on 24 August and then kept the central pressure of 945 hPa. However, the simulated typhoon continued to rapidly intensity till 1800 UTC on 25 August although the maximum wind speeds kept the value from 0000 UTC to 1200 UTC on 25 August (Figure 3c).

This study addresses the change in simulated central pressure and maximum surface winds during the mature phase. At 0600 UTC on 30 August, maximum surface winds increased and the increasing rate of simulated central pressure decreased. The time corresponded to the time when convective bursts were observed (Figure 1)

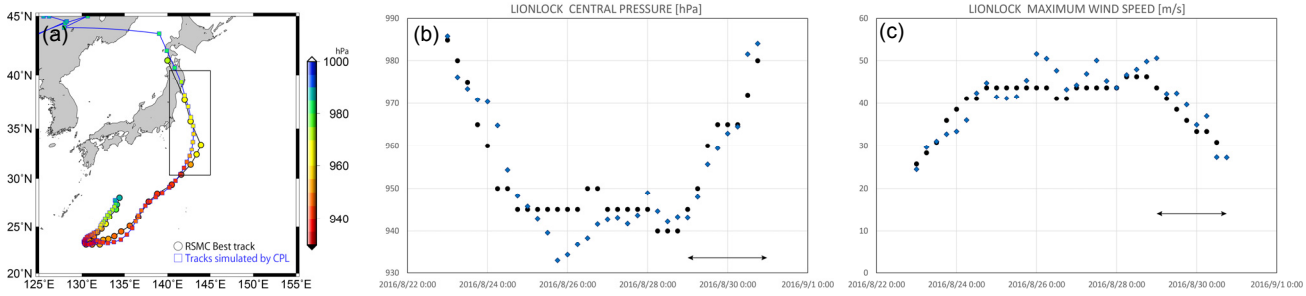

Figure 3 (a) Results of track simulations of Lionrock with simulated central pressures simulated by CPL together with RSMC best track data every three hours. (b) Time series of best track central pressures and central pressures simulated by CPL every six hours. (c) Same as (b) except for maximum wind speeds. Arrows in (b) and (c) indicated the period of mature phase that is focused on in this study.

3.2 Convective bursts and role of the ocean

Figure 4 shows more detailed time series of RSMC best track and simulated central pressure (Figure 4a) and maximum surface winds (Figure 4b) from 0000UTC on 29 August. The increasing rate of simulated central pressure decreased around 0600 UTC on 20 August, while keeping the maximum surface winds. Figure 5 shows the horizontal distributions of sea surface temperature (SST) with surface winds vectors and sea-level pressures at the interval of 4 hPa simulated by the CPL at 0000 UTC (Figure 5a) and 0600 UTC (Figure 5b) on 30 August. On the right hand side of the track of Lionrock, SST increased and the value was over 27 ˚C behind the typhoon due to near-inertial currents induced by the typhoon. The result suggests that the increase in SST was related to the decrease in the increasing rate of simulated central pressure.

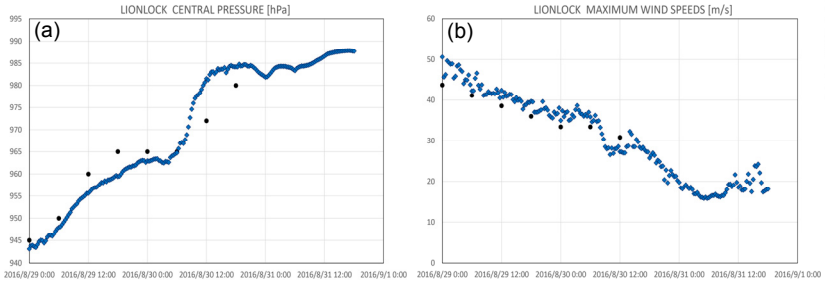

Figure 4 Same as Figure 3 except for the period from 0000UTC on 29 August at the interval of 20 minutes.

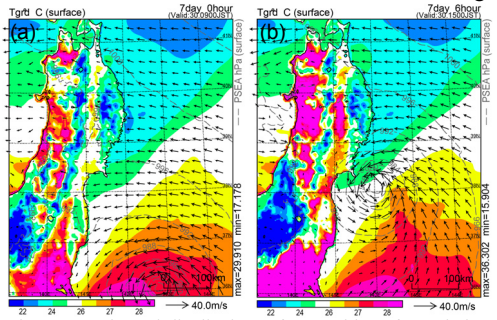

Figure 5 Horizontal distributions of SST with surface winds vectors and sea level pressures at the interval of 4 hPa simulated by the CPL at (a) 0000 UTC and (b) 0600 UTC on 30 August.

Figure 6 shows the horizontal resolution of total water content from the surface to ~17.5 km and the horizontal distributions of vertical velocity and potential vorticity at 8 km. Total water content was locally high at the quadrant of the moving direction of the storm. The high water-content area corresponded to the area where upward motion was locally dominant. This suggests that abundant water content was transported from the lower troposphere through locally strong upward motion. However, potential vorticity was relatively high in the inner core of the storm. In addition, potential vorticity was negative at the high water content area with locally strong upward vertical velocity. Thus convective bursts and associated cloud physics and dynamics contributed to the suppression of the dissipation. Thus, the storm could make landfall while keeping the intensity.

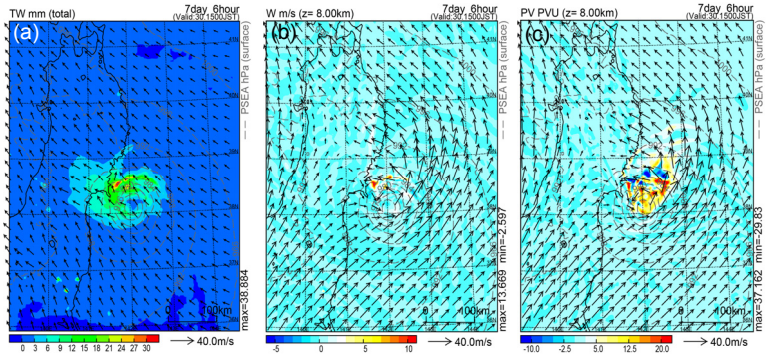

Figure 6 Same as Figure 5 except for (a) total water content from the surface to ~17.5 km with winds vectors at ~17.5 km, (b) vertical velocity with wind vectors at 8 km and (c) potential vorticity at 8 km with wind vectors at 8 km at 0600 UTC on 30 August.

4. Concluding remarks

This study addresses convective bursts occurred just before making landfall of Lionrock in the northern region of Japan. The numerical simulation performed by the CPL reasonably reproduced convective bursts at the quadrant of the moving direction of the typhoon. This feature was consistent with the observations. Warm water advected due to near-inertial currents enhanced by the storm was simulated at the timing of the decrease in the increasing rate of simulated central pressure. Convective bursts had locally high water content and negative potential vorticity, while potential vorticity was positive in the inner core of the storm.

These features were poorly simulated by a nonhydrostatic model with fixed SST given as a boundary condition although the simulated central pressure was extremely low (not shown). This implies that the oceanic response to Lionrock was related to the formation of convective bursts. Previous study using the same CPL reported that a similar rapid intensification occurred in the case of Typhoon Man-yi in 2013. Wada (2015) could not reproduce convective bursts realistically when the coupled model was used. The relation of convective bursts to rapid intensification and the dependence of the relation on geographical location will be a subject in the future as well as clarification of more detailed processes of convective bursts and their relation to typhoon-ocean interactions.

Acknowledgements

This work was supported by JSPS KAKENHI Grant Number JP15K05292.

References

Makihara Y (1996). A method for improving radar estimates of precipitation by comparing data from radars and raingauges. J Meteor Soc Japan 74:459-480.

Usui, N., S. Ishizaki, Y. Fujii, H. Tsujino, T. Yasuda and M. Kamachi (2006). Meteorological Research Institute multivariate ocean variational estimation (MOVE) system: Some early results. Advances in Space Research, 37(4), 806-822.

Wada A. (2015). Unusually rapid intensification of Typhoon Man-yi in 2013 under preexisting warm-water conditions near the Kuroshio front south of Japan. Journal of Oceanography, 71, 597–622.

Wada, A., N. Kohno and Y. Kawai (2010). Impact of wave-ocean interaction on Typhoon Hai-Tang in 2005. SOLA, 6A, 13-16.